JACS
JOURNAL OF THE AMERICAN CHEMICAL SOCIETY

ARTICLE

pubs.acs.org/JACS

Free-Standing Mesoporous Carbon Thin Films with Highly Ordered Pore Architectures for Nanodevices

Dan Feng, Yingying Lv, Zhangxiong Wu, Yuqian Dou, Lu Han, Zhenkun Sun, Yongyao Xia, Gengfeng Zheng,* and Dongyuan Zhao*

Department of Chemistry, Shanghai Key Laboratory of Molecular Catalysis and Innovative Materials, Laboratory of Advanced Materials, Fudan University, Shanghai 200433, People's Republic of China

Supporting Information

ABSTRACT: We report for the first time the synthesis of free-standing mesoporous carbon films with highly ordered pore architecture by a simple coating−etching approach, which have an intact morphology with variable sizes as large as several square centimeters and a controllable thickness of 90 nm to ∼3 μm. The mesoporous carbon films were first synthesized by coating a resol precursors/Pluronic copolymer solution on a preoxidized silicon wafer and forming highly ordered polymeric mesostructures based on organic−organic self-assembly, followed by carbonizing at 600 °C and finally etching of the native oxide layer between the carbon film and the silicon substrate. The mesostructure of this free-standing carbon film is confirmed to be an ordered face-centered orthorhombic *Fmmm* structure, distorted from the (110) oriented body-centered cubic $Im\bar{3}m$ symmetry. The mesoporosity of the carbon films has been evaluated by nitrogen sorption, which shows a high specific BET surface area of 700 m^2/g and large uniform mesopores of ∼4.3 nm. Both mesostructures and pore sizes can be tuned by changing the block copolymer templates or the ratio of resol to template. These free-standing mesoporous carbon films with cracking-free uniform morphology can be transferred or bent on different surfaces, especially with the aid of the soft polymer layer transfer technique, thus allowing for a variety of potential applications in electrochemistry and biomolecule separation. As a proof of concept, an electrochemical supercapacitor device directly made by the mesoporous carbon thin films shows a capacitance of 136 F/g at 0.5 A/g. Moreover, a nanofilter based on the carbon films has shown an excellent size-selective filtration of cytochrome *c* and bovine serum albumin.

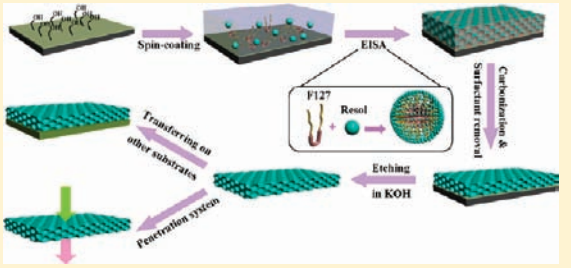

INTRODUCTION

Mesoporous carbon materials have attracted substantial attention due to their remarkable properties such as high specific surface area, ordered mesostructure, tunable pore size, low density, high conductivity, and chemical stability,[1−3] which possess great potentials for a variety of applications, such as adsorption,[4] hydrogen storage,[5] catalysis,[6] fuel cells,[7] and electrochemical supercapacitors.[8] The synthesis of ordered mesoporous carbon materials was previously achieved by the nanocasting method using mesostructured silica as a hard template.[9,10] Later, an amphiphilic surfactant templating method via organic−organic assembly based on the evaporation-induced self-assembly (EISA) process has been developed using amphiphilic block copolymers as structural-directing agents (templates).[1−3,11] By this route, ordered mesoporous carbon materials with tunable pore architectures and porosities have been obtained by using different organic template molecules and tuning the ratio of the carbon resol precursor and template.

From the view of practical applications, morphology control of mesoporous carbon materials is highly important. Various shapes and morphologies of mesoporous carbons, such as single crystals,[12] monoliths,[13] fibers,[13] nanospheres,[14] vesicles,[15] and films,[1,13,16−20] have been synthesized. Among these morphologies, thin films are unique candidates for applications in optical, electronic, electrochemical, and sensing devices and separation systems, due to their structure homogeneity and integrity.[21] Previously, the nanocasting method using mesoporous silica films as hard templates has been adopted to synthesize carbon film replica.[16,18] However, the mesoporous carbon films obtained by this method are discontinuous, probably due to the lack of mesopore connectivity in the silica film templates or the weak interaction between replica carbons and substrates. The most successful synthesis of mesoporous carbon films is based on the EISA mechanism via the organic−organic assembly of the carbon precursor with amphiphilic surfactants on substrates, followed by template decomposition and carbonization through thermal treatment.[1,13,17] Recently, we have demonstrated the synthesis of ordered mesoporous carbon films on silicon wafers with a variety of mesopore architectures based on EISA by using a phenol−formaldehyde oligomer as the precursor and a triblock copolymer as the template.[19,20]

To date, all of the mesoporous carbon films reported previously have been supported on certain solid substrates; however, due to the harsh conditions for carbonization, only several substrates with high thermal stability, such as silicon and mica, can be used to support mesoporous carbon films, thus limiting the

Received: June 17, 2011
Published: August 19, 2011

range of applications such as in polymer-based flexible substrates. Although the direct growth of free-standing mesostructured films from precursor solutions at the air−liquid or liquid−liquid interface, followed by the template removal, was reported to synthesize free-standing silica and organosilica films with different mesostructures,[22−29] this method is not suitable for the fabrication of free-standing mesoporous carbon films, as the film is brittle and is easily destroyed during the template removal or high-temperature carbonization. The successful synthesis of free-standing ordered mesoporous carbon films will provide many unique credentials. First, for the mesoporous carbons used as electrode materials, such as supercapacitors, free-standing thin films with three-dimensional (3-D) interconnected mesopores provide a continuous electron transport framework, low ion transport resistance, short electrolyte diffusion length, and the possibility of being transferred onto any substrates of interest, which can enlarge the range of conducting substrates and result in excellent electrochemical performance.[30] Second, although nanoscale porous materials have widely been employed in molecular infiltration,[31] it is difficult to directly apply this concept in mesoporous films, as the supporting substrate prohibits the transport of molecules through the thin films. Free-standing film morphology can serve as such a potential platform for protein separation. Moreover, the top and bottom surfaces of a free-standing film morphology can be asymmetrically functionalized and targeted, thus providing new devices such as directional ion transport.[32] Therefore, free-standing mesoporous carbon thin films are expected to lead to a variety of new opportunities in material designs and device applications.

Herein, we report the fabrication of free-standing mesoporous carbon thin films via a simple coating−etching method. First, phenolic resol precursors and Pluronic F127 block-copolymer templates have been mixed and spin-coated on a pretreated silicon wafer to form a highly ordered mesoporous carbon thin film via an organic−organic self-assembly process. Due to the existence of a native silica layer between the mesoporous carbon film and the silicon wafer, the carbon film can be separated from the substrate by etching off the intermediate silica layer. Through this route, for the first time, we have successfully synthesized an intact free-standing mesoporous carbon film with size as large as square centimeters and variable thickness from hundreds of nanometers to several micrometers. The mesopore architecture of the synthesized free-standing mesoporous carbon films has been investigated by cross-section transmission electron microscopy (TEM), high-resolution scanning electron microscopy (HR-SEM), and 2-D small-angle X-ray scattering (SAXS). The large porosity and the uniform pore size have been revealed by nitrogen sorption results. Moreover, the mesostructures and pore sizes of the free-standing carbon films are tunable, and the transferring process of the films can be facilitated by attaching a soft poly(methyl methacrylate) (PMMA) layer to the carbon film. Due to the highly ordered mesostructure, continuous electron transport framework, and capability of being transferred onto different substrates, these free-standing carbon films can be fabricated as functional devices as supercapacitors with excellent performance, exceeding that of their counterpart carbon materials, and biomolecule filter devices showing size-selective permeability for protein separation.

EXPERIMENTAL SECTION

Chemicals. Triblock copolymers, Pluronic F127 (poly(ethylene oxide)-*b*-poly(propylene oxide)-*b*-poly(ethylene oxide), EO_{106}-PO_{70}-EO_{106}, M_w = 12 600) and poly(methyl methacrylate) (PMMA, M_w = 996 000) were purchased from Sigma-Aldrich Corp. Other chemicals used for material synthesis were purchased from Shanghai Chemical Corp. All the reagents were used without further purification. Silicon wafers (Shanghai Xiangjing Corp.) with ⟨111⟩ surfaces were used as substrates.

Fabrication. Highly ordered mesoporous carbon thin films on silicon wafer substrate were synthesized via a simple coating method and the phenolic resol precursors and Pluronic F127 block copolymer employed as a carbon precursor and template, on the basis of the solvent evaporation induced organic−organic assembly process.[20] The silicon substrate was first treated with piranha solution (2/1 concentrated H_2SO_4/30% H_2O_2, v/v) at 90 °C for 30 min to clean the organic residues and form a thin native oxide layer on its surface. A water-soluble phenolic resol with a molecular weight of 500 was prepared by polymerizing phenol and formaldehyde using a base catalyst.[2] In a typical synthesis of the free-standing mesoporous carbon films, 0.33 g of homogeneous ethanol solution containing 0.06 g of resol, 0.03 g of Pluronic F127, and 0.24 g of ethanol was spin-coated on a pretreated silicon wafer (2×2 cm^2) at 4000 rpm for 60 s to form a thin film. The film was dried at room temperature for 5−8 h, followed by aging at 100 °C for 24 h (as-deposited film). A mesoporous carbon thin film on the silicon substrate was then obtained by pyrolyzing the as-deposited film at 600 °C for 3 h in nitrogen with a flow rate of 60 cm^3/min and a heating rate of 1 °C/min. Afterward, the obtained mesoporous carbon thin film on the silicon wafer was immersed into a potassium hydroxide (KOH) solution (10 wt %) at room temperature for 5−8 h to lift off the thin film. Then a free-standing carbon thin film with a size of 2×2 cm^2 and a thickness of ∼500 nm was obtained, which was carefully fished out and transferred into deionized water to wash three times. For comparison, mesoporous carbon powder (FDU-16) was also synthesized according the procedure reported by Meng et al.[2]

The free-standing film could be transferred onto other hard or soft substrates, such as metal, conductive glass, and paper. A layer of PMMA could be spin-coated on the top of the calcined mesoporous carbon film to enhance the flexibility of the thin film. For a typical transfer process, 0.3 mL of PMMA solution in anisole (10 wt %) was spin-coated on the top surface of a presynthesized mesoporous carbon film on silicon wafer (2×2 cm^2) at 2000 rpm for 30 s, followed by solvent evaporation at room temperature for 1 h and then baking with the substrate at 115 °C for 15 min. Afterward, using the aforementioned etching and washing conditions, a free-standing PMMA/mesoporous carbon composite film was obtained. After the composite thin film was transferred onto a new substrate, the PMMA layer was removed by immersing the composite film in acetone for 2 h.

Characterization. Optical photos were taken by a Canon A1100IS camera (Japan). X-ray diffraction (XRD) patterns were collected with a Bruker D4 powder X-ray diffractometer (Germany) using Cu Kα radiation (40 kV, 40 mA). The d spacing values were calculated using the formula $d = \lambda/2(\sin\theta)$. Small-angle X-ray scattering (SAXS) patterns were recorded with a Nanostar U small-angle scattering system (Bruker, Germany) using Cu Kα radiation (40 kV, 35 mA). The free-standing carbon films were either directly attached to the sample holder and placed vertical to the path of the incident X-ray or cut into small pieces (∼5 mm^2) and randomly filled into the hole on the sample holder (Supporting Information, Scheme S1). The as-deposited film was scraped off from the substrate, ground into powder, and filled into the hole on the sample holder for SAXS measurements. 2-D SAXS patterns were directly obtained, while the linear patterns were obtained by full integration of diffraction dots. The d spacing values were calculated using the formula $d = 2\pi/q$, where $q = 4\pi(\sin\theta)/\lambda$. High-resolution scanning electron microscopy (HR-SEM) images were obtained on a Hitachi S4800 field-emission SEM (Japan) operated at 1 kV and 10 μA. Transmission electron microscopy (TEM) measurements were conducted on a JEOL 2100F microscope (Japan) at 200 kV. Films for cross-section TEM analysis were embedded in epoxide resin and then cut by

Scheme 1. Schematic Representation of the Preparation Process for Free-Standing Mesoporous Carbon Thin Films with Highly Ordered *Fmmm* Mesostructure by Using a Coating−Etching Approach[a]

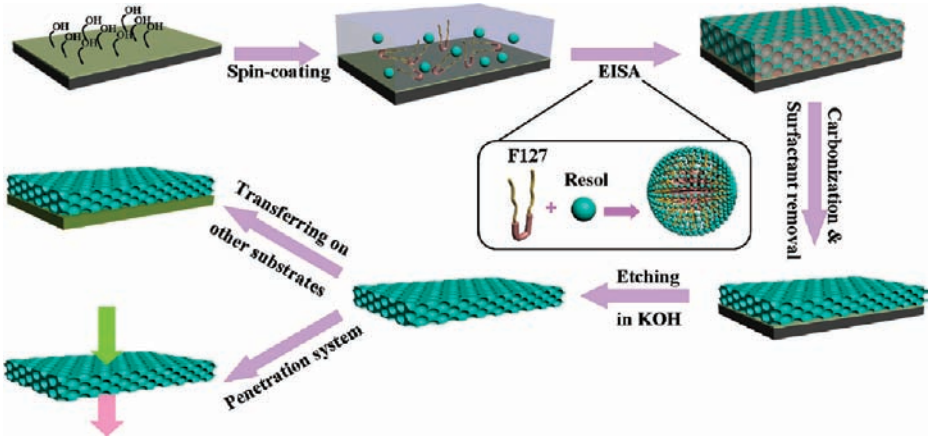

[a] The coating process of the mesoporous carbon film on a pretreated silicon wafer with a native silica top layer is based on the organic−organic assembly of resol and Pluronic F127, followed by carbonization at 600 °C. Then, the etching of the ultrathin native silica layer occurs when the carbon film with the substrate is put into a concentrated KOH solution, resulting in a free-standing mesoporous carbon film separated from the silicon wafer substrate. Legend: (black region) silicon wafer; (gray region) ultrathin silica layer; (light blue region) ethanol solution; (green/red region) mesostructured polymer/F127 composite; (green region) mesoporous carbon film; (light green region) new substrate.

an ultracut microtome with a diamond knife. The obtained slices were supported on a carbon-coated copper grid. Furthermore, the films were also smashed by ultrasonic dispersion in ethanol and dropped on a carbon-coated copper grid for TEM observations. The thickness of the free-standing carbon film was measured using a Dektak 150 surface profiler (Veeco, USA). Nitrogen sorption isotherms were measured using a Micromeritics Tristar 3000 analyzer at −196 °C. Before the measurement was taken, the free-standing films were ground into powders and then degassed at 180 °C for 6 h. The Brunauer−Emmett−Teller (BET) method was utilized to calculate the specific surface area (S_{BET}) using the adsorption data at p/p_0 = 0.05−0.25. The pore size distribution (PSD) was derived from the adsorption branch by using the Barrett−Joyner−Halenda (BJH) model. The total pore volume (V_{total}) was estimated from the adsorbed amount at p/p_0 = 0.99.

Electrochemical Measurements. The electrochemical device as a supercapacitor was made by placing a free-standing mesoporous carbon thin film on a nickel foil serving as the current collector. Cyclic voltammetry and galvanostatic charge/discharge cycling tests of the thin film based device were measured on a CHI 606B electrochemical analyzer system (Shanghai CHI Instruments Co.) under ambient conditions. A three-electrode glass cell with 6 M KOH electrolyte was used, in which Pt foil was used as the counter electrode and an Hg/HgO electrode (0.052 V vs the normal hydrogen electrode, NHE) as the reference electrode. Specific capacitances (C) were calculated by the equation $C = I(\Delta t)/m(\Delta U)$, where I is the discharge current (mA), Δt is the total discharge time (s), m is the total mass of active material in both electrodes (g), and ΔU is the potential difference during the discharging (V).

Protein Filtration and Separation. The filter device based on the free-standing mesoporous carbon film was made by first transferring a film and placing it between two layers of cellulose acetate/cellulose nitrate (CA-CN) membranes with 400 nm pores, followed by sealing them in a filter holder. An aqueous solution containing 1.0×10^{-5} M cytochrome c (cyt c) and 1.0×10^{-5} M bovine serum albumin (BSA) was injected into the filter device. The solution that permeated through the thin film was collected. The composition changes of the protein mixture solutions before and after the filtration were determined by UV−vis absorption spectra using a JASCO V-550 spectrophotometer.

RESULTS AND DISCUSSION

Fabrication. The new coating−etching route for synthesis of free-standing mesoporous carbon thin films is described in Scheme 1. Briefly, a pretreated silicon wafer with a native silica top layer serves as a substrate for spin-coating the resin/surfactant precursors. When the solvent is evaporated, the organic−organic assembly occurs,[2] in which the Pluronic F127 triblock copolymers and phenolic resols form a composite mesostructured thin film (as-deposited film on the substrate), with spherical surfactant micelles surrounded by resin frameworks. This as-deposited film is heated under an inert atmosphere to decompose the triblock copolymers at 300−400 °C, while the phenolic resin is carbonized at 600 °C to form a mesoporous carbon thin film. The integrity of the thin films is well retained, due to the confinement and supporting effect of the substrate. Then, the carbon film with the silicon wafer substrate is put into a concentrated KOH solution and the ultrathin native silica layer is quickly etched, leading to a free-standing mesoporous carbon film separated from the silicon wafer substrate.

The optical image (Figure 1a) shows the macroscopic morphology of a typical free-standing mesoporous carbon film directly removed from the silicon substrate. This free-standing thin film is black and intact with an area around 2 × 2 cm^2. In comparison to the mesoporous carbon film on silicon wafer (Supporting Information, Figure S1a), the free-standing thin film retains the same size and shape as the former on the substrate. The film size can be readily scaled up to any size of silicon wafer substrate, but the mechanical strength of the free-standing films may decrease with the film thickness. While floating in water (Figure 1a), the free-standing mesoporous carbon thin film can be unfurled with a slight curvature and easily fished out and transferred onto different substrates. The SEM image (Figure 1b) shows that the free-standing films are continuous and smooth without any cracks. The films have a uniform thickness around 500 nm, confirmed by both the SEM and surface profiler results. The thickness of the mesoporous carbon films can be tuned from

90 to 3000 nm by varying the concentrations of the precursor solution for the coating process (Table S1). Our results show that films thicker than 3000 nm are less uniform due to the high-viscosity precursor solution, while films thinner than 100 nm are fragile due to the amorphous carbon composition as well as the large porosity.

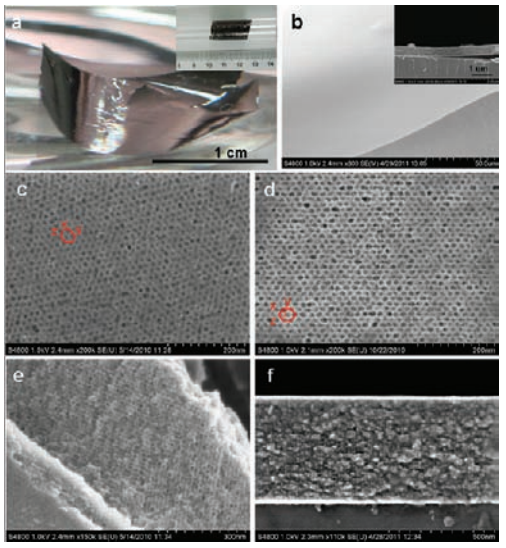

Figure 1. (a) Optical photo of a free-standing mesoporous carbon film floating in water (the inset shows the free-standing carbon film transferred onto a cylindrical substrate). (b) SEM images of the free-standing mesoporous carbon films (the inset shows a cross-section). High-resolution SEM images of (c) the top surface, (d) the bottom surface, (e) the edge part from (c), and (f) a cross-section of the free-standing mesoporous carbon films after pyrolysis at 600 °C in N_2. The cross-section observations were carried out by transferring the free-standing films onto a silicon wafer followed by placing the substrate vertically at the edge of the sample holder.

Mesostructure and Porosity. HR-SEM images (Figure 1c,d) demonstrate that, after being removed from substrates, both top and bottom surfaces of the free-standing carbon films have well-ordered hexagonal-shaped arrays of mesopores, in which the lattice shapes and scales are similar to the top surface of the original mesoporous carbon film on the silicon substrate (Figure S1c). The side lengths of the distorted hexagon lattice are measured by SEM images to be $x = y = 0.865z$, and the angle between x and z is about 109.5°, implying the top surface of an orthorhombic *Fmmm* structure with the (010) planes parallel to the substrate, which is distorted from a (110)-oriented $Im\bar{3}m$ mesostructure (Scheme 2). We should note that other space groups with lower symmetry, such as *F*222 *and Fmm*2, are also possible, as these space groups are not distinguishable from the extinction conditions. Here we take the highest symmetry of *Fmmm*, which is the most understandable.[33] Although the (010) planes are uniformly oriented, the films are not "single-crystal" mesostructures but are composed of crystal-like mesostructured domains with (010) orientations and sizes of several hundred nanometers (Figure S1c). HR-SEM images of the edge part and cross-section of the free-standing mesoporous carbon films (Figure 1e,f) also show highly ordered mesopore architectures. Therefore, both the macroscale and microscale morphologies of the mesoporous carbon films are well retained during the etching process.

Cross-section TEM images of the free-standing mesoporous carbon film (Figure 2a,b) show a distorted hexagonal lattice, in accordance with the calculated model (Scheme 2), which is a typical lattice of mesostructure with space group *Fmmm* symmetry viewed from the [101] direction. The *d* value of (020) planes measured from TEM images is around 5 nm, consistent with the result calculated from the XRD pattern of the mesoporous carbon film on the substrate (Figure S1b). The pore size is roughly measured from TEM images to be around 4 nm, consistent with mesopores generated by Pluronic F127 spherical micelles in an amorphous carbon framework.[2] Moreover, when

Scheme 2. Schematic Representation of (a) Structural Conversion of a Mesostructured Carbonaceous Film from (110)-Oriented Cubic $Im\bar{3}m$ to *Fmmm* Mesostructure during the Pyrolysis, as well as the Lattices on the Top Surface (b) and on Cross Section (c) of *Fmmm* Symmetry

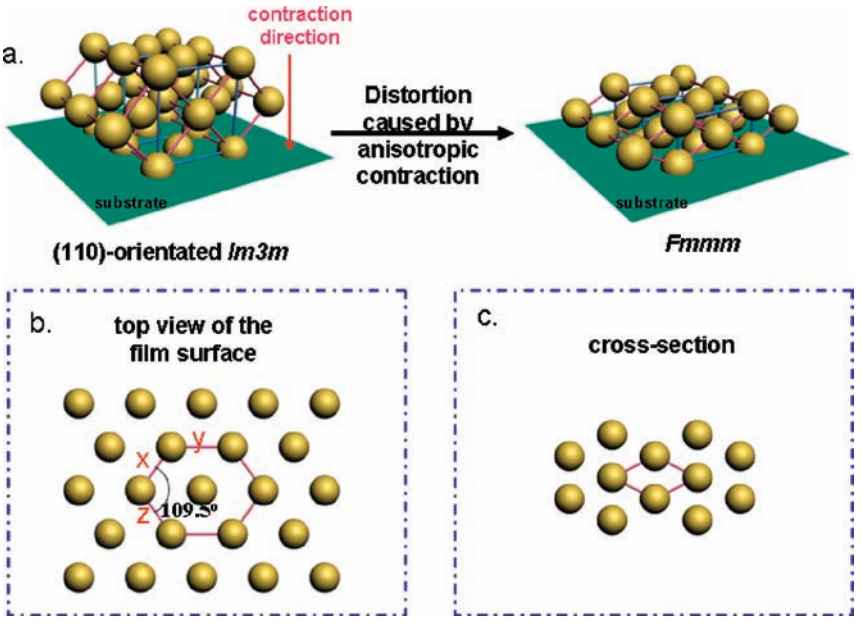

dx.doi.org/10.1021/ja2056227 |*J. Am. Chem. Soc.* 2011, 133, 15148–15156

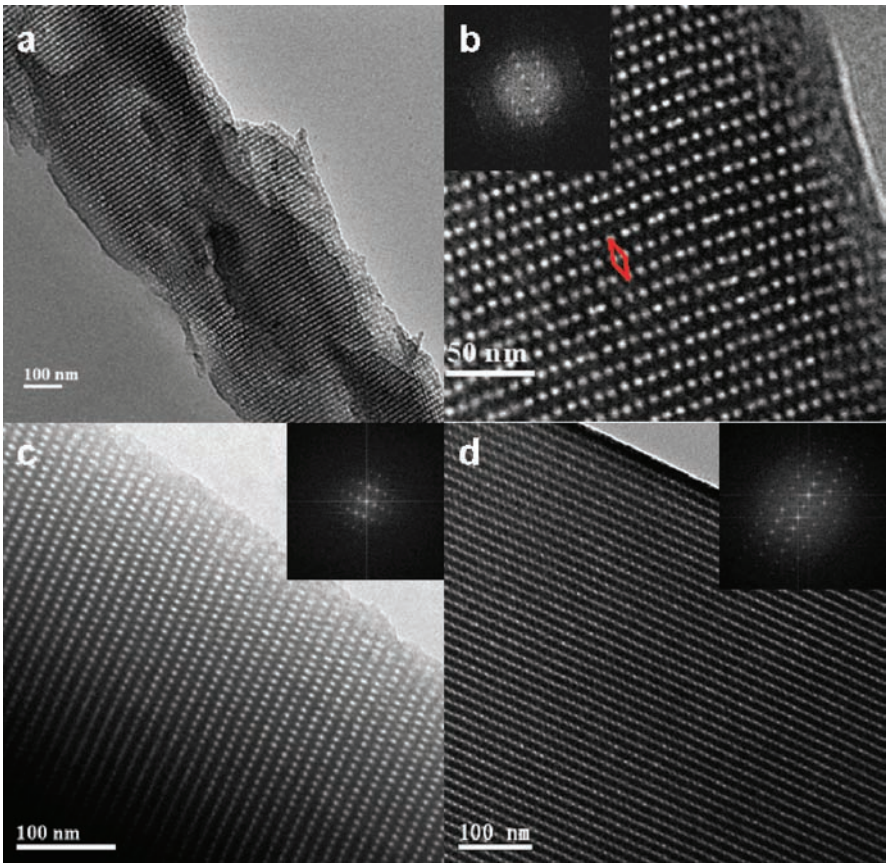

Figure 2. Cross-section TEM images (a, b) and TEM images (c, d) of the free-standing mesoporous carbon films along (c) the $[10\bar{1}]$ zone axis and (d) the [010] zone axis. Insets (b−d) are the corresponding FFT patterns (see the indexation of FFT patterns and schematic representations in Figure S2). The cross-section TEM analysis was carried out by embedding a free-standing film in epoxide resin, cutting it by an ultracut microtome, and then supporting the obtained slices on a carbon-coated copper grid.

the free-standing carbon films are ground into powder, TEM images (Figure 2c,d) demonstrate typical lattices of a *Fmmm* symmetry incident along the $[10\bar{1}]$ and [100] zone axes, which further confirms the mesostructure of the films. The unit cell parameters measured by TEM images and the indexed FFT patterns (Figure S2) are a = 19.0 nm, b = 10.0 nm, and c = 26.8 nm.

The SAXS pattern of the as-deposited film (before the pyrolysis, being ground into a powder for the measurement) (Figure S3a) clearly shows five well-resolved diffraction peaks, associated with the 110, 200, 211, 310, and 321 reflections of 3-D body-centered symmetry with the cubic space group of $Im\bar{3}m$. This is in good accordance with that of the bulk as-made FDU-16 materials (Figure S3b),[2] suggesting a similar mesostructure. Furthermore, d values of the as-made film and powder calculated from the 110 scattering peaks are both 13.8 nm. The 1-D integral curve of the free-standing mesoporous carbon films (Figure 3a, lower curve) shows a series of well-resolved diffraction peaks, which can be attributed to the 002, 200, 202, 004, 400 reflections of a *Fmmm* symmetry in accordance with the calculated results from FFT patterns (Figure S2), suggesting a highly ordered mesostructure. However, the d spacing value of the free-standing mesoporous carbon film calculated from the 002 peak and 200 peak (13.8 and 10.0 nm, respectively, indicating c = 27.6 nm and a = 20.0 nm) is much larger than that of the 110 peak of bulk FDU-16 carbon materials (∼9.4 nm, indicating the unit cell parameter a = 13.3 nm) (Figure 3a, upper curve), and the relative intensities of the diffraction peaks for the films and bulk materials are different. This is attributed to the orientation of the mesoporous carbon films and the distorted mesostructure caused by anisotropic contraction during pyrolysis. Furthermore, in comparison to the FDU-16 powder, the more resolved diffraction peaks of the film sample can be probably attributed to the higher ordering resulting from the strong interfacial interaction during the EISA process of forming very thin layers.

Further evidence for the orientation can be obtained from 2D-SAXS patterns of the free-standing mesoporous carbon thin films. Two ways have been used for collecting 2-D diffraction information on the free-standing films (Scheme S1). According to the measurement in Scheme S1a, an intact free-standing thin film was placed vertical to the incident direction. No diffraction rings or dots were observed around a 2θ value of 1.8°, corresponding to the (020) planes of *Fmmm* symmetry. The disappearance of the diffraction at the 2θ value of 1.8° indicates that the (020) planes are oriented normal to the film surface. For other planes, several diffraction rings are observed in the 2-D SAXS pattern (Figure 3b), implying a "polycrystalline" film composed of (010)-oriented crystal-like domains (Scheme S1a). When the free-standing films were cut into small pieces and randomly filled into the hole for SAXS measurements (Scheme S1b), diffraction dots at a 2θ angle of 1.8° with a d spacing value of 4.9 nm could be observed (Figure 3c, illustrated in Scheme S1b), indicating the unique orientation of (020)

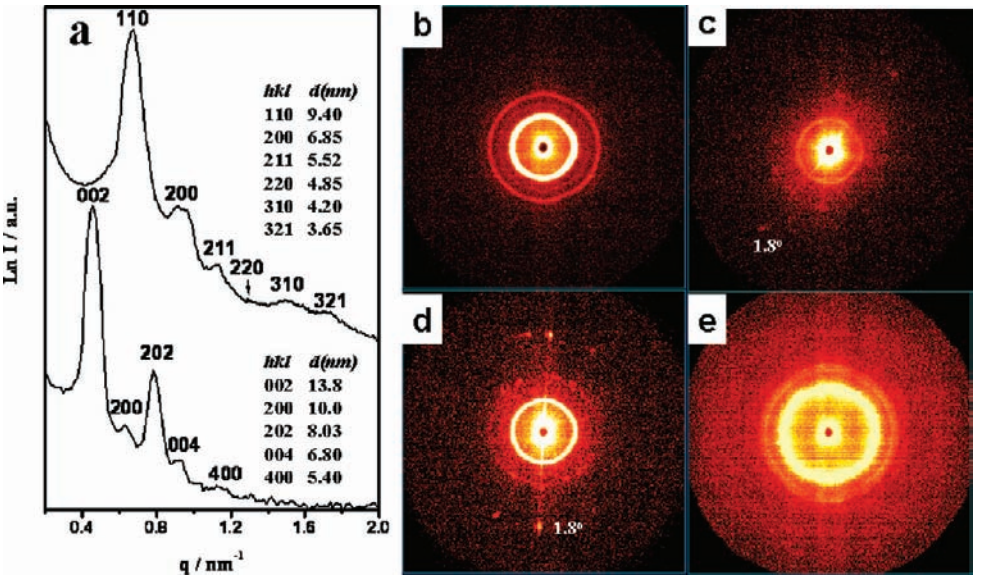

Figure 3. (a) SAXS integral curves of (lower curve) the free-standing mesoporous carbon films (pyrolyzed at 600 °C) placed vertical to the incident light path and (upper curve) bulk mesoporous carbon FDU-16 powder (pyrolyzed at 600 °C). 2-D SAXS patterns (b−e) of an intact free-standing mesoporous carbon film vertical to the incident light path (b), small pieces of free-standing carbon film (∼5 mm^2) (c, d), and bulk FDU-16 carbon powder sample (e).

planes of *Fmmm* in the films. All (020) planes in one film piece should be oriented in only one direction, though they may belong to different domains. Filling more pieces of film for the SAXS measurements can decrease the characteristics of 2-D diffraction patterns and lead to more averaged results (Figure 3d). For comparison, a 2-D SAXS pattern of the isotopic FDU-16 powder shows symmetric rings (Figure 3e).

The nitrogen sorption isotherm of the free-standing mesoporous carbon films after pyrolysis at 600 °C (Figure 4) shows a typical type IV curve with a hysteresis loop and a distinct condensation step, indicating a uniform large cagelike mesopore architecture. The surface area (S_{BET}) and the pore volume (V_{total}) are calculated to be as high as 700 m^2/g and 0.46 cm^3/g, respectively, which are comparable to the values for mesoporous carbon FDU-16 powder pyrolyzed in nitrogen at 600 °C (690 m^2/g and 0.44 cm^3/g).[34] Moreover, there is a narrow pore size distribution (inset in Figure 4), indicating the uniform mesopores of the carbon films. The pore size calculated from the adsorption branch is ∼4.3 nm, while the window size calculated from the desorption branch is ∼3.5 nm, in accordance with the pore size value measured from TEM images. These results indicate an excellent porosity of the free-standing mesoporous carbon films, including high surface area, large pore volume, and uniform mesopores, which can be attributed to the well-ordered mesostructure via the organic−organic self-assembly and thermal stability of the cross-linked pore walls.

The structure and porosity of the free-standing mesoporous carbon thin films can be controlled by varying the synthesis conditions. The mesostructure can be varied by simply changing the ratio of the resol precursor and triblock copolymer (F127) template. Our results show that the free-standing mesoporous carbon films with an orthorhombic *Fmmm* symmetry are formed when the weight ratio of resol to F127 is 2:1. When the weight ratio of resol to F127 is changed to 1.5:1, it generates a 2-D hexagonal mesostructure with a *p6m* symmetry for the as-deposited film and a distorted structure with a *c2m* symmetry

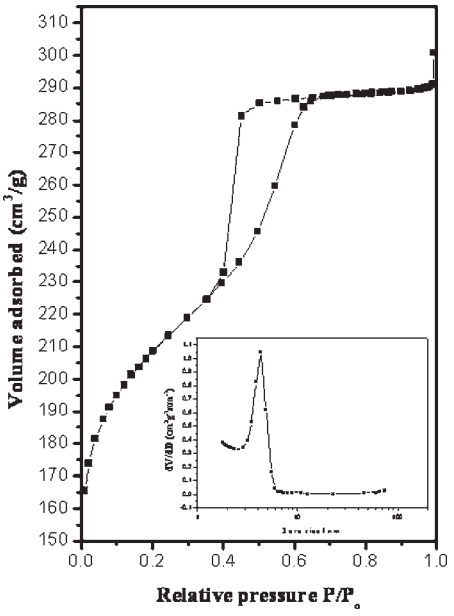

Figure 4. Nitrogen sorption isotherm and corresponding pore size distribution curve (inset) of the free-standing mesoporous carbon films after pyrolysis at 600 °C.

for the free-standing carbon film, in which the cylindrical channels are parallel to the film surface (Figure S4a). The pore sizes of the free-standing mesoporous carbon films can be tuned by changing block copolymer templates. For example, by using a diblock copolymer of polystyrene-*b*-poly(ethylene oxide) (PS_{180}-*b*-PEO_{125}, M_w = 23 000) as a template, a free-standing carbon film with ∼20 nm spherical mesopores can be synthesized (Figure S4b). Furthermore, double-layer free-standing mesoporous carbon films with different pore sizes can be synthesized via repeated coating of different precursor solutions,

dx.doi.org/10.1021/ja2056227 |*J. Am. Chem. Soc.* 2011, 133, 15148–15156

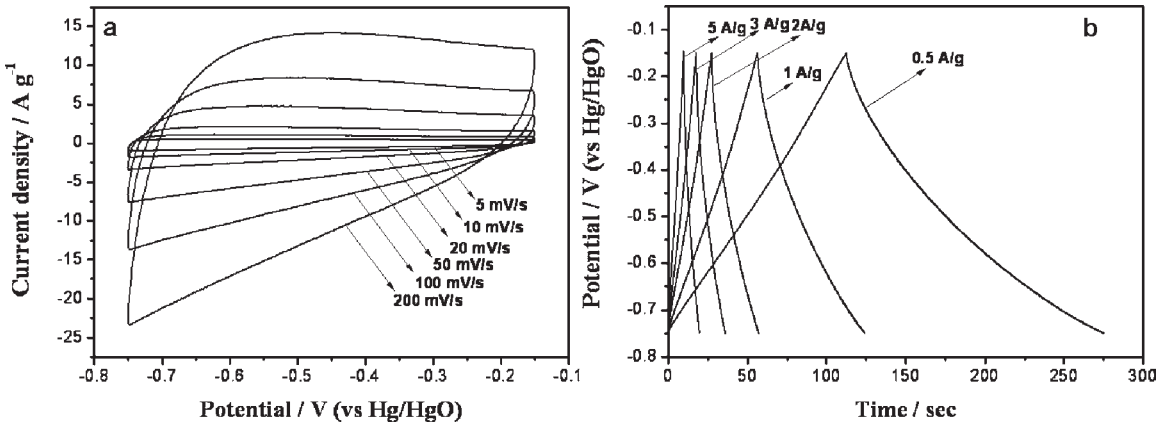

Figure 5. (a) Cyclic voltammograms at various scan rates and (b) charge−discharge curves at different current densities of the free-standing mesoporous carbon film after being pyrolyzed at 600 °C.

followed by pyrolysis and silica etching (Figure S4c−e). The thicknesses of both the top and bottom layers can be individually tuned from 90 to 3000 nm, typically around 500 nm (Figure S4c). Templated by the diblock copolymer PS_{180}-*b*-PEO_{125} and the triblock copolymer F127 for each layer, the obtained double-layered free-standing carbon film has well-ordered mesopores with openings around 20 and 8 nm on the top and bottom surfaces, respectively (Figure S4d,e).

In addition, to further enhance the flexibility and portability of the free-standing mesoporous carbon films, a soft polymer layer assisted transfer method has been developed (Scheme S2). First, a PMMA layer (∼300 nm) can be spin-coated over the top surface of the mesoporous carbon film on a silicon substrate. After etching of the native oxide of the silicon substrate, the composite PMMA/mesoporous carbon double-layer film morphology can be well preserved and transferred to another substrate even with large curvatures, such as a cylindrical shape (inset in Figure 1a). The PMMA layer can be easily dissolved by acetone. The free-standing mesoporous carbon thin film synthesized by this polymer layer assisted transfer method does not show any observable change in the SAXS pattern (Scheme S2a), indicating that the PMMA coating does not affect the mesostructure of the carbon film and can be used as a good supporting layer for film transfer. This PMMA-layer assisted technique facilitates transferring the free-standing films onto any substrate of interest for device fabrication.

Electrochemical Supercapacitor Device. Mesoporous carbon has been widely utilized for electrode materials in electrochemical devices such as batteries and supercapacitors.[30] Typically, carbon samples are in powder morphologies; thus, the electrical conductivity is limited and different binders such as poly(tetrafluoroethlyene) are required.[35] By transferring the obtained free-standing mesoporous carbon films onto an electrode collector (i.e., a nickel foil), we can easily fabricate a new type of thin-film working electrode in supercapacitor devices without binders, conductive additives, or post-compression molding.

The cyclic voltammogram (CV) at a low scan rate of 5 mV/s (Figure S5a) shows a rectangular shape, suggesting a typical double-layer capacitance behavior. When the scan rate is increased from 5 to 200 mV/s (Figure 5a), a similar rectangular shape is retained, indicating a good capacitive performance at high scan rates. The charge−discharge cycling tests of the free-standing mesoporous carbon thin film based electrochemical devices were conducted at current densities from 0.5 to 5 A/g. Charge−discharge curves at different current densities (Figure 5b) all show isosceles triangular shapes, suggesting excellent Coulombic efficiency and ideal capacitor behavior. No sudden potential drop is observed, revealing that this mesoporous carbon thin film based electrochemical device has low equivalent series resistance (ESR). The specific capacitance is calculated from the charge−discharge curve to be ∼136 F/g at a current density of 0.5 A/g, similar to that of cubic structured mesoporous carbon FDU-16 powders and much larger than that of mesoporous carbon films with similar porosity previously reported.[35,36] The capacitance could be further enhanced by introducing other components, such as nitrogen and conducting polymers, to form hybrid materials.[37,38] When the current density is increased to 5 A/g, it exhibits a specific capacitance of 85 F/g (Figure S5b). The decrease of specific capacitance at large current densities is possibly due to the orthorhombic structure of the carbon films with cage-like mesopores, in which fast electrolyte diffusion is hindered at the windows among pores. This phenomenon was also found in supercapacitors based on the mesoporous carbon powders with cage-like pores.[35] Although the specific capacitance decreases as the current density is increased, due to the cage-like pore structures, the specific capacitance of the thin film based devices is maintained at about 63% at 5 A/g, indicating a rate capability better than that of the mesoporous carbon powders with comparable porosity and structure.[35] The excellent performance of this supercapacitor is attributed to the continuous carbon framework in the film that facilitates electron transport and avoids electron hopping among different particles in powders. In addition, the anisotropic contraction of the films during the pyrolysis enhances the connectivity of mesopores along the vertical direction, and the thin thickness shortens the distance of electrolyte ion diffusion. These results demonstrate the possibility of fabricating nanodevices based on free-standing mesoporous carbon thin films for electrochemical applications.

Nanofiltration Device for Protein Separations. Due to the enhanced penetrating property across the films and the high chemical stability, the obtained free-standing mesoporous carbon films can be used as filtration membranes for protein separation based on the size selectivity of uniform mesopores with comparable sizes to large biomolecules. A typical nanofilter device is prepared by placing a free-standing mesoporous carbon thin film between two layers of CA-CN membranes (∼ 400 nm pores)

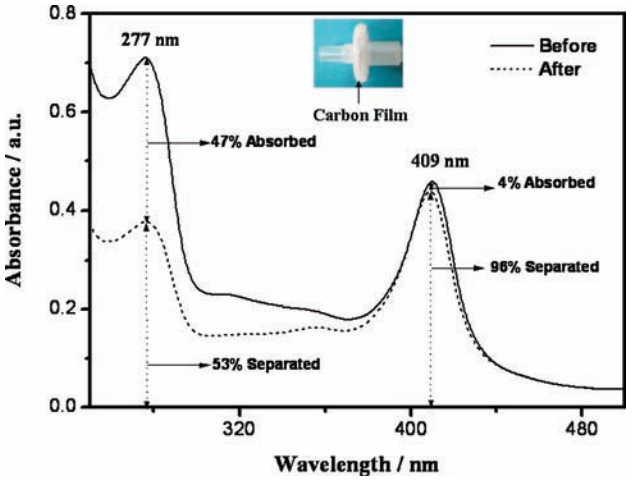

Figure 6. UV−vis absorption spectra before and after filtering a mixture solution of 1.0×10^{-5} M cyt *c* and 1.0×10^{-5} M BSA through the free-standing mesoporous carbon thin film based nanofilter device (the inset gives an optical photo of the nanofilter device).

and sealing them in a filter holder (Figure 6, inset). The separation property of this device is evaluated by filtering a mixed aqueous solution of two proteins, cytochrome *c* (cyt *c*) and bovine serum albumin (BSA).

Figure 6 shows the UV−vis spectra of a solution mixture of cyt *c* and BSA proteins before and after the filtration, where the absorption peaks at 409 and 277 nm are attributed to cyt *c* and BSA, respectively. The molecular sizes of cyt *c* and BSA are $2.5 \times 2.5 \times 3.7$ and $4.0 \times 4.0 \times 14.0$ nm, respectively. As for cyt *c* with a spherical size smaller than the mesopore window, the peak at 409 nm decreases slightly after the filtration, indicating that 96% of cyt *c* can permeate through the carbon film filter. In contrast, a 47% decrease of absorbance at 277 nm is observed, indicating that only 53% of BSA can permeate through the film. The difference in protein permeability is attributed to the size-selective effect of the uniform mesopores. Cyt *c* with smaller size can diffuse through the carbon mesopores with only a slight loss, probably due to the adsorption over the pore surfaces. However, the BSA molecule has one dimension (~14.0 nm) that is much longer than the mesopore window; thus, a significant amount (~47%) of the molecules can be blocked by the carbon film filter. Those BSA molecules diffusing through the carbon film may be attributed to the molecule orientation and slight defects among structural domains. Therefore, the designed nanofilter based on the free-standing mesoporous carbon thin films shows good selectivity of different proteins and can serve as a separation system. It is expected that the selectivity of protein permeation can be optimized by tailoring the pore sizes and architecture, which provides a new platform for a wide range of proteins and other biomolecules separated by this thin film device.

CONCLUSIONS

This work is the first report of synthesizing free-standing carbon thin films with highly ordered mesopore architecture by a simple coating−etching route. The obtained free-standing carbon film has a highly ordered face-centered orthorhombic *Fmmm* mesostructure, high specific surface area, uniform mesopore sizes, and an intact morphology of over several square centimeters. By control of the types and concentrations of both surfactants and resol precursors, mesoporous carbon films with tunable thickness, architectures, and multiple layers have been realized. In addition, we have developed a PMMA layer assisted transfer method to enhance the film flexibility and portability and have demonstrated the device application of these free-standing carbon thin films as a electrochemical capacitor and a nanofilter for separation of proteins. This synthesis method is simple and convenient and can be readily applied to a variety of other material compositions as free-standing films with diverse mesopore architectures, thus opening up a host of opportunities of developing new functional nanodevices.

ASSOCIATED CONTENT

Supporting Information. Figures and a table giving schematic diagrams of the SAXS measurements for the free-standing mesoporous carbon films and the PMMA-assisted transfer technique, optical photos, XRD patterns, and HR-SEM images of mesoporous carbon films on substrates, indexation of FFT patterns of TEM images, SAXS patterns of as-deposited film and as-made powder, HR-SEM images of free-standing carbon films with different mesostructures and pore sizes, and cyclic voltammetry curves at a low scan rate and specific capacitance variation with various charge/discharge current densities. This material is available free of charge via the Internet at http://pubs.acs.org.

AUTHOR INFORMATION

Corresponding Author

*E-mail: dyzhao@fudan.edu.cn (D.Z.); gfzheng@fudan.edu.cn (G.Z.). Tel: 86-21-5163-0205. Fax: 86-21-5163-0307.

ACKNOWLEDGMENT

This work was supported by the NSF of China (No. 20890123), the State Key Basic Research Program of the PRC (Nos. 2009AA033701 and 2009CB930400), Science and Technology Commission of Shanghai Municipality (No. 08DZ2270500), and Shanghai Leading Academic Discipline Project (No. B108). We greatly appreciate the financial supports from Delta Environmental & Educational Foundation (Taiwan).

REFERENCES

(1) Liang, C. D.; Hong, K. L.; Guiochon, G. A.; Mays, J. W.; Dai, S. *Angew. Chem., Int. Ed.* **2004**, *43*, 5785.
(2) Meng, Y.; Gu, D.; Zhang, F.; Shi, Y.; Yang, H.; Li, Z.; Yu, C.; Tu, B.; Zhao, D. *Angew. Chem., Int. Ed.* **2005**, *44*, 7053.
(3) Tanaka, S.; Nishiyama, N.; Egashira, Y.; Ueyama, K. *Chem. Commun.* **2005**, 2125.
(4) Wu, Z. X.; Zhao, D. Y. *Chem. Commun.* **2011**, *47*, 3332.
(5) Wu, Z. X.; Yang, Y. X.; Gu, D.; Zhai, Y. P.; Feng, D.; Li, Q.; Tu, B.; Webley, P. A.; Zhao, D. Y. *Top. Catal.* **2009**, *52*, 12.
(6) Joo, S. H.; Choi, S. J.; Oh, I.; Kwak, J.; Liu, Z.; Terasaki, O.; Ryoo, R. *Nature* **2001**, *412*, 169.
(7) Chai, G. S.; Yoon, S. B.; Yu, J. S.; Choi, J. H.; Sung, Y. E. *J. Phys. Chem. B* **2004**, *108*, 7074.
(8) Simon, P.; Gogotsi, Y. *Nat. Mater.* **2008**, *7*, 845.
(9) Ryoo, R.; Joo, S. H.; Jun, S. *J. Phys. Chem. B* **1999**, *103*, 7743.
(10) Ryoo, R.; Joo, S. H.; Kruk, M.; Jaroniec, M. *Adv. Mater.* **2001**, *13*, 677.
(11) Zhang, F.; Meng, Y.; Gu, D.; Yan, Yu, C.; Tu, B.; Zhao, D. *J. Am. Chem. Soc.* **2005**, *127*, 13508.

(12) Gu, D.; Bongard, H.; Meng, Y.; Miyasaka, K.; Terasaki, O.; Zhang, F.; Deng, Y.; Wu, Z.; Feng, D.; Fang, Y.; Tu, B.; Schüth, F.; Zhao, D. *Chem. Mater.* **2010**, *22*, 4828.
(13) Liang, C. D.; Dai, S. *J. Am. Chem. Soc.* **2006**, *128*, 5316.
(14) Fang, Y.; Gu, D.; Zou, Y.; Wu, Z.; Li, F.; Che, R.; Deng, Y.; Tu, B.; Zhao, D. *Angew. Chem., Int. Ed.* **2010**, *49*, 7987.
(15) Gu, D.; Bongard, H.; Deng, Y. H.; Feng, D.; Wu, Z. X.; Fang, Y.; Mao, J. J.; Tu, B.; Schüth, F.; Zhao, D. Y. *Adv. Mater.* **2010**, *22*, 833.
(16) Pang, J. B.; Li, X.; Wang, D. H.; Wu, Z. W.; John, V. T.; Yang, Z. Z.; Lu, Y. F. *Adv. Mater.* **2004**, *16*, 884.
(17) Tanaka, S.; Katayama, Y.; Tate, M. P.; Hillhouse, H. W.; Miyake, Y. *J. Mater. Chem.* **2007**, *17*, 3639.
(18) Lin, M. L.; Huang, C. C.; Lo, M. Y.; Mou, C. Y. *J. Phys. Chem. C* **2008**, *112*, 867.
(19) Song, L. Y.; Feng, D.; Campbell, C. G.; Gu, D.; Forster, A. M.; Yager, K. G.; Fredin, N.; Lee, H. J.; Jones, R. L.; Zhao, D. Y.; Vogt, B. D. *J. Mater. Chem.* **2010**, *20*, 1691.
(20) Song, L. Y.; Feng, D.; Fredin, N. J.; Yager, K. G.; Jones, R. L.; Wu, Q. Y.; Zhao, D. Y.; Vogt, B. D. *ACS Nano* **2010**, *4*, 189.
(21) Nicole, L.; Boissiere, C.; Grosso, D.; Quach, A.; Sanchez, C. *J. Mater. Chem.* **2005**, *15*, 3598.
(22) Aksay, I. A.; Trau, M.; Manne, S.; Honma, I.; Yao, N.; Zhou, L.; Fenter, P.; Eisenberger, P. M.; Gruner, S. M. *Science* **1996**, *273*, 892.
(23) Tolbert, S. H.; Schaffer, T. E.; Feng, J. L.; Hansma, P. K.; Stucky, G. D. *Chem. Mater.* **1997**, *9*, 1962.
(24) Fernandez-Martin, C.; Roser, S. J.; Edler, K. J. *J. Mater. Chem.* **2008**, *18*, 1222.
(25) Yang, B.; Edler, K. J. *Chem. Mater.* **2009**, *21*, 1221.
(26) Park, S. S.; Park, D. H.; Ha, C. S. *Chem. Mater.* **2007**, *19*, 2709.
(27) Park, S. S.; Ha, C. S. *Chem. Mater.* **2005**, *17*, 3519.
(28) Park, S. S.; Shin, J. H.; Zhao, D. Y.; Ha, C. S. *J. Mater. Chem.* **2010**, *20*, 7854.
(29) Yang, H.; Coombs, N.; Sokolov, I.; Ozin, G. A. *Nature* **1996**, *381*, 589.
(30) Liu, C.; Li, F.; Ma, L. P.; Cheng, H. M. *Adv. Mater.* **2010**, *22*, E28.
(31) El-Safty, S. A.; Shahat, A.; Warkocki, W.; Ohnuma, M. *Small* **2011**, *7*, 62.
(32) Hou, X.; Guo, W.; Jiang, L. *Chem. Soc. Rev.* **2011**, *40*, 2385.
(33) Innocenzi, P.; Malfatti, L.; Kidchob, T.; Falcaro, P. *Chem. Mater.* **2009**, *21*, 2555.
(34) Meng, Y.; Gu, D.; Zhang, F. Q.; Shi, Y. F.; Cheng, L.; Feng, D.; Wu, Z. X.; Chen, Z. X.; Wan, Y.; Stein, A.; Zhao, D. Y. *Chem. Mater.* **2006**, *18*, 4447.
(35) Sun, G.; Wang, J.; Liu, X.; Long, D.; Qiao, W.; Ling, L. *J. Phys. Chem. C* **2010**, *114*, 18745.
(36) Dai, M.; Song, L.; LaBelle, J. T.; Vogt, B. D. *Chem. Mater.* **2011**, *23*, 2869.
(37) Fan, L. Z.; Hu, Y. S.; Maier, J.; Adelhelm, P.; Smarsly, B.; Antonietti, M. *Adv. Funct. Mater.* **2007**, *17*, 3083.
(38) Zhao, L.; Fan, L. Z.; Zhou, M. Q.; Guan, H.; Qiao, S.; Antonietti, M.; Titirici, M. M. *Adv. Mater.* **2010**, *22*, 5202.